

Evaluation of the Adaptive Statistical Iterative Reconstruction Algorithm in Chest CT (Computed Tomography) A Preliminary Study toward Its Employment in Low Dose Applications, Also in Conjunction with CAD (Computer Aided Detection)

Patrizio Barca^{1,2,3}, Federica Palmas^{1,3}, Maria Evelina Fantacci^{1,3} and Davide Caramella⁴

¹Department of Physics, University of Pisa, Pisa, Italy

²Unit of Medical Physics, Pisa University Hospital "Azienda Ospedaliero-Universitaria Pisana", Pisa, Italy

³INFN, Pisa Section, Pisa, Italy

⁴Department of Radiology, Pisa University Hospital "Azienda Ospedaliero-Universitaria Pisana", Pisa, Italy

Keywords: Chest Computed Tomography, Image Quality, Modulation Transfer Function, Noise Power Spectrum, Contrast.

Abstract: Lung cancer is one of the leading cause of cancer death worldwide. Computed Tomography (CT) is the best imaging modality for the detection of small pulmonary nodules and for this reason its employment as a screening tool has been widely studied. However, radiation dose delivered in a chest CT examination must be considered, especially when potentially healthy people are examined in screening programs. In this context, iterative reconstruction (IR) algorithms have shown the potential to reduce image noise and radiation dose and computer aided detection (CAD) systems can be employed for supporting radiologists. Thus, the combined use of IR algorithms and CAD systems can be of practical interest. In this preliminary work we studied the potential improvements in the quality of phantom and clinical chest images reconstructed through the Adaptive Statistical Iterative Reconstruction (ASIR, GE Healthcare, Waukesha, WI, USA) algorithm, in order to evaluate a possible employment of this algorithm in low dose chest CT imaging with CAD analysis. We analysed both clinical and phantom CT images. Noise, noise power spectrum (NPS) and modulation transfer function (MTF) were estimated for different inserts in the phantom images. Image contrast and contrast-to-noise ratio (CNR) of different nodules contained in clinical chest images were evaluated. Noise decreases non-linearly when increasing the ASIR blending level of reconstruction. ASIR modified the NPS. The MTF for ASIR-reconstructed images depended on tube load, contrast and blending level. Both image contrast and CNR increased with the ASIR blending level.

1 INTRODUCTION

Lung cancer is one of the most frequently diagnosed cancers and the leading causes of cancer death in men worldwide (Malvezzi et al., 2015; Siegel et al., 2015). In fact, most of lung cancer cases are diagnosed in the late stages when the survival rate is very low. An early detection considerably improves the survival rate and for this reason the implementation of screening programs is of relevant interest. The best diagnostic tool for the detection of pulmonary nodules is Computed Tomography (CT) and its employment in screening trials has shown great results in terms of reduced mortality (The National Lung Screening Trial Research Team, 2011). An additional tool that can be helpful in lung

cancer screening is represented by computer aided detection (CAD) systems. In fact, many studies have shown satisfactory results in terms of sensitivity and specificity (Lopez Torres et al., 2015; Fantacci et al., 2017), so as CAD systems can be employed to reduce radiologist workload and improving the quality of chest CT scan interpretation in screening examinations. However, in order to minimise the risk of radiation induced cancer in patients (potentially healthy in screening examinations) low-dose CT is required. Recent advances in CT technology include different methods of dose optimisation and reduction (Goo, 2012). In particular, iterative reconstruction algorithms (IR) show the potential of improving image quality in low-dose image acquisitions as compared to

standard filtered back-projection (FBP) reconstruction (Willeminck et al., 2013). Therefore, IR algorithms could be employed in low-dose CT examinations preserving the diagnostic quality of images (which conversely is degraded when FBP reconstruction is adopted). For this reason, recent works were focused on combining IR methods with CAD systems (Huber et al., 2016; Yoon et al., 2015; Wielpütz et al., 2015; Harder et al., 2016). These studies showed that in many clinical situations low-dose chest CT with IR algorithms does not significantly worsen the CAD sensitivity obtained with standard chest CT and conventional FBP reconstruction. However, some studies have shown that image quality obtained through iterative reconstruction depends on image contrast and radiation dose (Richard et al., 2012; Samei et al., 2015). Thus, more insights on the performance of IR algorithms for chest examinations can be of practical interest.

In a previous phantom study, we assessed the image quality performance of a CT scanner (Optima CT660, GE Healthcare, Waukesha, WI, USA) which implements the Adaptive Statistical Iterative Reconstruction (ASIR, GE Healthcare, Waukesha, WI, USA) algorithm (Barca et al., 2017). We performed a systematic analysis of noise, contrast-to-noise ratio (CNR) and spatial resolution by varying the main exposure parameters in a wide range of values and testing the ASIR's performance on different image contrasts. We demonstrated that a relevant noise reduction and CNR increment in CT images can be achieved with the ASIR algorithm with respect to the conventional FBP reconstruction. Additionally, spatial resolution decreases with increasing the ASIR blending level of reconstruction for low dose acquisitions and low contrast objects. However, only a quality control protocol was adopted in image acquisition without any clinical and only phantom images were analysed.

In this study, we investigate potential strengths of the ASIR algorithm in terms of image quality that could be of practical interest in conjunction with lung CAD system at low and very low radiation exposure levels. We study the dependence of different image quality parameters on the ASIR-FBP blending level of reconstruction, both in phantom and clinical chest images. The analysis performed in the previous work was repeated to characterise the quality of images obtained through ASIR in a 128-slice CT scanner (Discovery 750 HD, GE Healthcare, Waukesha, WI, USA). However, while in the previous study images were acquired through scan protocols often used in quality controls, in this

analysis we employed a clinical chest scan protocol to acquire the phantom images. Then, we focused our attention on clinical chest acquisitions of patients with pulmonary nodules, whose images were retrospectively reconstructed using different ASIR-FBP blending levels; we studied noise and contrast properties of these images in order to evaluate the employment of ASIR and its effect on nodule detectability.

2 MATERIALS AND METHODS

Images of the Catphan-504 phantom (The Phantom Laboratory, NY, USA) were acquired on the Discovery 750-HD CT using a scan protocol routinely adopted in chest CT examinations (Table 1) and varying the main exposure parameters in a wide range of values (Specifically, four values of tube voltage and eight values of tube load were employed: 80, 100, 120 and 140 kVp, 32¹, 63, 84, 105, 126, 147, 168, 189 mAs). The Catphan-504 phantom is composed of 4 modules with cylindrical shape (internal diameter of 15 cm). We employed the CTP486 module (a homogeneous water-equivalent module) and the CTP404 module (composed of many inserts of different materials in a water-equivalent background).

Image quality was evaluated through the assessment of noise, noise power spectrum (NPS) and modulation transfer function (MTF).

Noise and NPS were computed from images of the CTP486 phantom section while for MTF assessment we employed images of the CTP404 phantom section.

Noise was measured by computing the standard deviation (σ) of Hounsfield units (HU) within a region of interest (ROI), while for the NPS assessment we adopted the Siewerdsen et al. approach: we computed the 3D NPS and then we obtain a radial representation of the 3D NPS by selecting the $f_z=0$ plane of the 3D NPS and performing an average of several radial profiles.

The MTFs were derived following the circular edge method through edge spread function (ESF) measurements (Richard et al., 2012; Samei et al., 2015). ESFs were referred to six different inserts of the CTP404 section (air, PMP, LDPE, polystyrene,

¹ In order to evaluate the spatial resolution performance of the ASIR algorithm at low radiation exposure, a set of images of the CTP404 section were acquired at 32 mAs (lowest value used in our analysis). This value was only employed for MTF evaluation.

delrin and teflon).

Additionally, images of patients that underwent chest CT clinical examinations were anonymised and retrospectively reconstructed² using different ASIR-FBP blending levels (from 20% to 100%). In these images, nodules of different sizes (4 mm to 7 mm) were identified, then, the CNR and the percentage contrast were computed. The CNR was estimated as follows:

$$CNR = \frac{HU_{nodule} - HU_{background}}{\sqrt{\sigma_{nodule}^2 + \sigma_{background}^2}} \quad (1)$$

where $HU_{nodule} / \sigma_{nodule}$ and $HU_{background} / \sigma_{background}$ are the mean/standard deviation of HU values in a circular ROI in the considered nodule and background region. The percentage contrast was defined by the following formula:

$$C(\%) = \frac{HU_{nodule} - HU_{background}}{HU_{background}} 100\% \quad (2)$$

Uncertainties associated to data values were computed as standard deviations of repeated measurements. For some measurements this approach was not possible (e.g. for contrast analysis in clinical images). However, we tested the reproducibility of our measurements adopting the clinical chest scan protocol and computing the coefficient of variation (COV) from a set of ten acquisitions. The COV resulted <0.03 for each

ASIR-FBP blending level employed in the reconstruction process.

Image data analysis was performed using ImageJ (Wayne Rasband, National Institute of Health, USA) and Matlab (The MathWorks, Inc., USA) software packages.

Table 1: Standard chest scan protocol routinely adopted in the Discovery 750-HD CT machine for chest examinations.

Scan protocol	standard chest
Modality	helical
Tube load	126 mAs
Tube voltage	100 -120 *kVp
Pitch	0.984:1
Slice thickness	2.5 mm
S-FOV	M Body
D-FOV	220 mm
Collimation width	40 mm

*The kVp value could be set to 100 kVp or 120 kVp depending on the patient size.

3 RESULTS

Figure 1 shows the noise obtained varying tube load and tube voltage for conventional FBP algorithm and ASIR with different blending levels of reconstruction (20%, 40%, 60%, 80%, 100%). Noise decreased non-linearly with the increase of ASIR blending level of reconstruction as well as with increasing tube load and tube voltage.

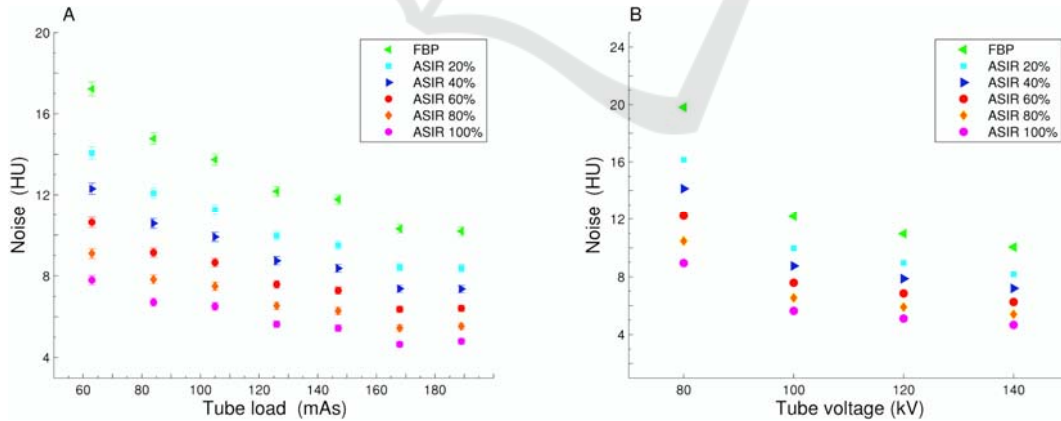


Figure 1: Noise (standard deviation) for conventional FBP algorithm and different ASIR blending levels of reconstruction (20%, 40%, 60%, 80%, 100%) with varying tube load (panel A) and tube voltage (panel B). Other parameters of acquisition were set as in Table 1.

² These images were acquired with the standard chest protocol (Table 1) and first reconstructed with FBP.

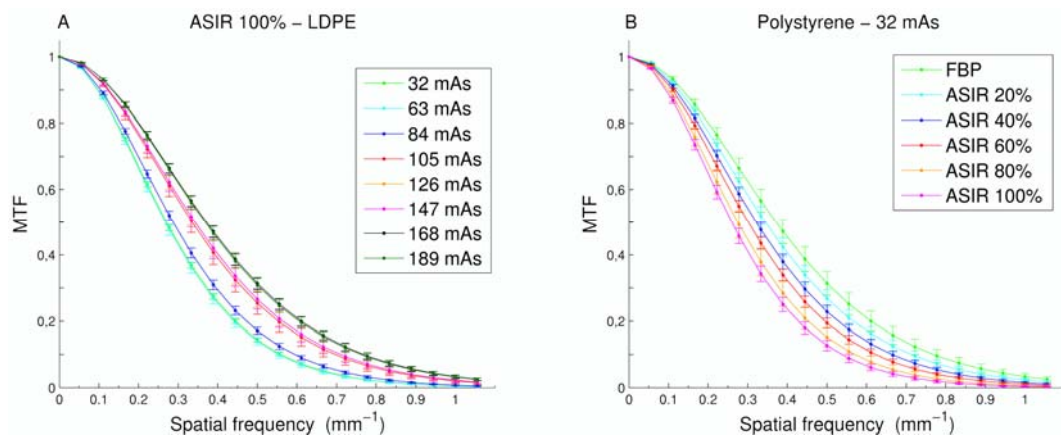


Figure 3: MTF for ASIR-reconstructed CT images (blending level of 100%) and medium-low (LDPE) contrast level, with varying tube load (panel A). MTF for low (32 mAs) tube load and low (polystyrene) contrast CT images, with varying reconstruction methods.

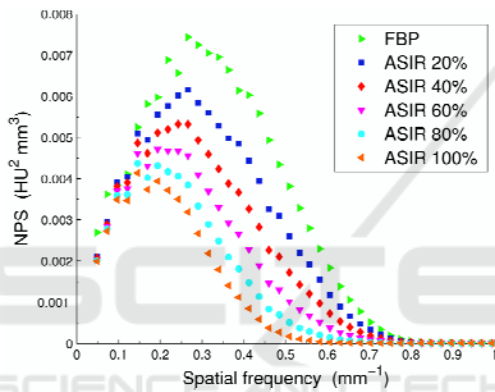


Figure 2: Radial NPS for conventional FBP algorithm and ASIR algorithm with different blending levels of reconstruction. Images were acquired adopting the chest scan protocol of Table 1.

Results about NPS are reported in Figure 2. ASIR algorithm acts as a low pass filter whose effect increases with the increase of blending level of reconstruction.

Results about spatial resolution are reported in Figures 3 and 4. For ASIR-reconstructed CT images and low contrast level, the MTF decreased with decreasing tube load (Fig. 3 A). The MTF of ASIR-reconstructed CT images varied even with the contrast level (Fig. 4), especially at low tube load. In particular, the MTF decreased with decreasing contrast level. While for high contrast objects or high tube load values ASIR preserves the spatial resolution obtained by FBP reconstruction, for medium (e.g. 126 mAs, which is the value adopted in the standard chest protocol on the Discovery 750-HD CT) and low (e.g. 32 mAs, the lowest value that was employed in our study) tube load and contrast

level, the MTF of ASIR-reconstructed CT images was lower than the MTF of conventional FBP-reconstructed images, and the first decreased with increasing blending level of reconstruction (Fig. 3 B).

Figure 5 shows one example of clinical image containing a nodule of 5 mm. Examples of the CNR and percentage contrast results are reported in Figures 6 and 7 for nodules of 4, 5 and 6 mm of diameter. CNR and percentage contrast of the nodules increased non-linearly with increasing the ASIR level of reconstruction (up to 43% and 9% respectively).

4 DISCUSSIONS

In this study we evaluated CT image quality through the assessment of different indexes related to noise (noise and NPS), contrast (CNR and percentage contrast) and spatial resolution (MTF) properties of phantom and clinical images, comparing the performance of two different reconstruction technologies.

As expected, our findings confirm the noise reduction potential of the ASIR algorithm. Specifically, when compared to FBP, ASIR can reduce image noise up to 55 % (Figure 1), showing the potential of image quality improvement at low radiation exposures. Furthermore, it seems that ASIR acts as a non-linear low-pass filter, which can modify noise texture and affect spatial resolution especially at low contrast and low radiation exposure when medium/high blending levels of reconstruction are employed (Figures 2 and 3).

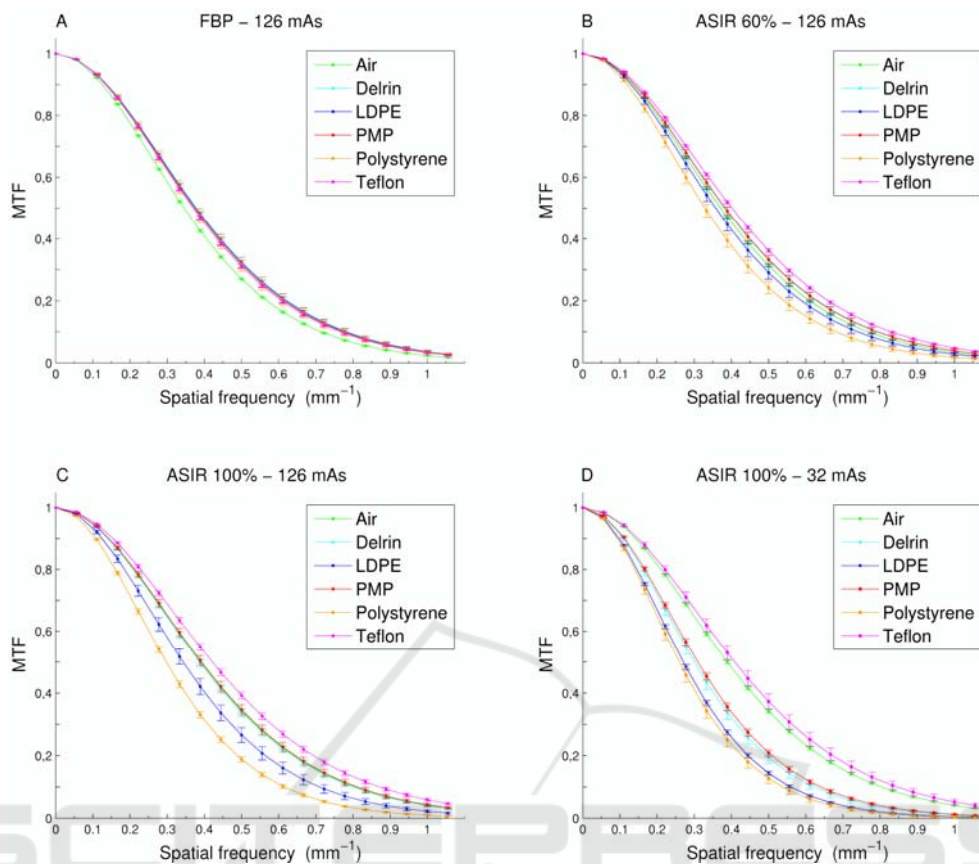


Figure 4: MTF for ASIR-reconstructed CT images (blending level of reconstruction of 0% (panel A), 60% (panel B) and 100% (panels C and D) and medium (126 mAs, panel A, B and C) /low (32 mAs, panel D) tube load.

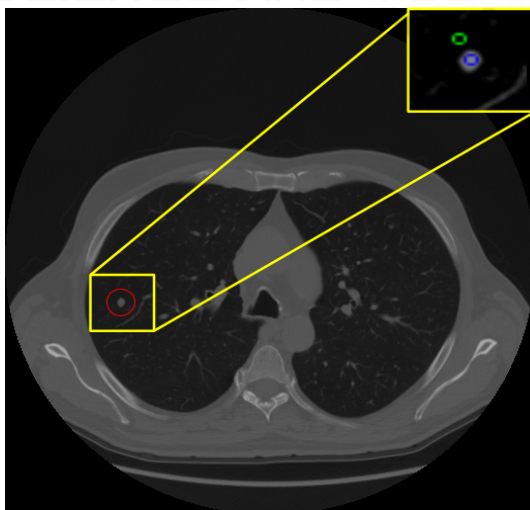


Figure 5: Example of a pulmonary nodule (5 mm of diameter) employed for CNR and percentage contrast evaluation (The ROI in green represented the “background ROI”, while the ROI in blue represented the “nodule ROI”).

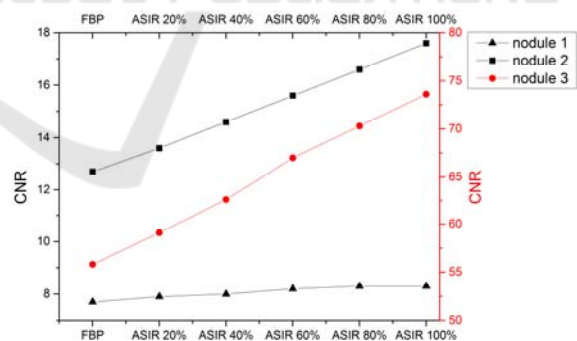


Figure 6: Examples of CNRs for nodules of 4 mm (nodule 1), 5 mm (nodule 2) and 6 mm (nodule 3) of diameter. Clinical images were acquired adopting the chest scan protocol of Table 1.

In addition, chest clinical images reconstructed with ASIR exhibit interesting properties in terms of increased CNR and percentage contrast of small nodules (Figures 6 and 7). These results are in agreement with previous qualitative studies in which the detection of lesions seems to be improved when

the ASIR algorithm is employed in the reconstruction process instead of the conventional.

FBP (Willeminck et al., 2013). Another study highlighted that a 50% ASIR-FBP blending level allowed to maintain acceptable CNR and image noise levels in low-dose images of different chest phantoms (Mathieu et al, 2014). The authors showed that, as compared to conventional FBP, radiation dose could be reduced by 40% by using 50% ASIR-FBP blending level of reconstruction without affecting overall image quality.

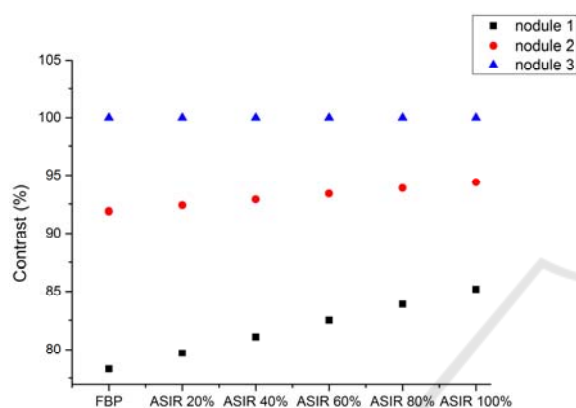


Figure 7: Examples of percentage contrasts for nodules of 4 mm (nodule 1), 5 mm (nodule 2) and 6 mm (nodule 3) of diameter. Clinical images were acquired adopting the chest scan protocol of Table 1.

As shown in our results, the quality of ASIR-reconstructed images is strictly related to the blending level of reconstruction. However, even though the choice of the ASIR-FBP blending level is extremely important to avoid losses in details detection, ASIR images exhibit considerably better noise and contrast properties as compared to FBP images. Notice that while the CNR increment may be due to the noise reduction performed by ASIR, the percentage contrast is not directly related to image noise (Eq. 2). This means that ASIR could also improve tissue differences in terms of HU values and thus have positive influences on CAD performances. Therefore, the ASIR algorithm may be employed in low-dose chest CT acquisitions (which are required in screening examinations) and in combination with CAD systems as suggested by previous studies (Hyun et al, 2015). It should be reminded that spatial resolution with ASIR reconstruction depends also on radiation dose and on the objects contrast in the images (Figures 3 and 4). These dependences should be carefully considered in order to evaluate and optimise the combined employment of ASIR and the CAD system available

for us (Torres et al., 2015; Fantacci et al., 2017) for pulmonary nodules detection in ultra-low dose conditions.

5 CONCLUSIONS

In this work we assessed the noise, contrast and spatial resolution properties of phantom and human chest CT images reconstructed through different ASIR-FBP blending levels.

An important noise reduction and CNR increment is achieved in images reconstructed through the ASIR algorithm. Percentage contrast also increases with the blending level of reconstruction. For these reasons ASIR may be employed in low-dose chest CT examinations and it could positively influence CAD performances. However, since spatial resolution decreases with the increasing of the blending level of reconstruction in low dose acquisitions, this parameter should be carefully optimised.

Even though further studies are needed, our findings provide additional insights into the characterisation of the ASIR algorithm performance and can be of practical interest toward an its adequate employment.

REFERENCES

- Barca P, Giannelli M, Fantacci ME and Caramella D. 2017. Evaluation of the Imaging Properties of a CT Scanner with the Adaptive Statistical Iterative Reconstruction Algorithm; *Proceedings of Proceedings of BIOSTEC 2017, Bioinformatics, Biodevices*; 200-206
- Catphan ® 504 Manual - The Phantom Laboratory (NY, USA).
- Den Harder AM, Willeminck MJ, van Hamersvelt RW, Vonken EPA, Milles J, Schilham AMR, Lammers JW, de Jong PA, Leiner T, Budde RPJ. 2016. Effect of radiation dose reduction and iterative reconstruction on computer aided detection of pulmonary nodules: Intra individual comparison. *European Journal of Radiology*; 85:346-351
- Fantacci ME, Traverso A, Bagnasco S, Bracco C, Campanella D, Chiara G, Lopez Torres E, Manca A, Regge D, Saletta M, Stasi M, Vallero S, Vassallo and Cerello P. 2017. A Web- and Cloud- based Service for the Clinical Use of a CAD (Computer Aided Detection) System, *Proceedings of BIOSTEC 2017, Bioinformatics*; 202-209
- Goo H W. 2012. CT Radiation Dose Optimization and Estimation: an Update for Radiologists, *Korean Journal of Radiology*; 13(1):1-11

- Huber A, Landau J, Ebner L, Bütikofer Y, Leidolt L, Brela B, May M, Heverhagen and Christe A. 2016. Performance of ultralow-dose CT with iterative reconstruction in lung cancer screening: limiting radiation exposure to the equivalent of conventional chest X-ray imaging, *European Radiology*; 26(10):3643-52
- Hyun JY, Myung JC, Hye SH, Jung WM and Kyung SL. 2015. Adaptive Statistical Iterative Reconstruction-Applied Ultra-Low-Dose CT with Radiography-Comparable Radiation Dose: Usefulness for Lung Nodule Detection. *Korean Journal of Radiology*; 16(5):1132-41
- Lopez Torres E, Fiorina E, Pennazio F, Peroni C, Saletta M, Camarlinghi N, Fantacci ME and Cerello P. 2015. Large scale validation of the M5L lung CAD on heterogeneous CT datasets, *Medical Physics*; 42(4):1477-89
- Malvezzi M, Bertuccio P, Rosso T, Rota M, Levi F, La Vecchia C and Negri E. 2015. *Annals of Oncology*; 26:779-786
- Mathieu KB, Ai H, Fox PS, Godoy MCB, Munden RF, de Groot PM, Pan T. 2014. Radiation dose reduction for CT lung cancer screening using ASIR and MBIR: a phantom study, *Journal of applied clinical medical Physics*; 15(2):271-80
- Richard S, Husarik DB, Yadava G, Murphy SN, Samei E. 2012. Towards task-based assessment of CT performance: system and object MTF across different reconstruction algorithms. *Medical Physics*; 39(7):4115-22
- Samei E and Richard S. 2015. Assessment of the dose reduction potential of a model-based iterative reconstruction algorithm using a task-based performance metrology. *Medical Physics*; 42(1):314-23
- Siegel R L, Miller K D and Jemal A. 2015. *CA: a cancer journal for clinicians*; 65:5-29
- Siewerdsen JH, Cunningham IA and Jaffray DA. 2002. A framework for noise-power spectrum analysis of multidimensional images. *Medical Physics*; 29(11):2655-71
- Mathieu KB, Ai H, Fox PS, Godoy MCB, Munden RF, de Groot PM, Pan T. 2014. Radiation dose reduction for CT lung cancer screening using ASIR and MBIR: a phantom study, *Journal of applied clinical medical Physics*; 15(2):271-80
- The National Lung Screening Trial Research Team. 2011. Reduced lung cancer mortality with low dose computed tomographic screening, *The New England Journal of Medicine*; 365(5):395-409
- Wielpütz MO, Wroblewski J, Lederlin M, Dinkel J, Eichinger M, Koenigkam-Santos M, Biederer J, Kauczor HU, Puderbach MU and Jobst BJ. 2015. Computer-aided detection of artificial pulmonary nodules using an ex vivo lung phantom: influence of exposure parameters and iterative reconstruction. *European Journal of Radiology*; 84:1005-1011
- Willemink MJ, de Jong PA, Leiner T, de Heer LM, Nievelstein RA, Budde RP, Schilham AM. 2013. Iterative reconstruction techniques for computed tomography Part 1: Technical principles. *European Radiology*; 23:1623-31.